

# Hadron production in deuteron-gold collisions and nuclear parton distributions

Adeola Adedoyi and George Fai  
*Center for Nuclear Research, Department of Physics*  
*Kent State University, Kent, OH 44242, USA*  
 (Dated: February 9, 2022)

We calculate nuclear modification factors  $R_{dAu}$ , central-to-peripheral ratios,  $R_{CP}$ , and pseudorapidity asymmetries  $Y_{Asym}$  in deuteron-gold collisions at  $\sqrt{s} = 200$  GeV in the framework of leading-order (LO) perturbative Quantum Chromodynamics. We use the Eskola-Kolhinen-Salgado (EKS), the Frankfurt-Guzey-Strikman (FGS) and the Hirai-Kumano-Nagai (HKN) nuclear parton distribution functions and the Albino-Kramer-Kniehl (AKK) fragmentation functions in our calculations. Results are compared to experimental data from the BRAHMS and STAR collaborations.

PACS numbers: 24.85.+p, 25.30.Dh, 25.75.-q

## I. INTRODUCTION

In the rapidly-developing field of relativistic nuclear collision physics, questions related to the distribution of partons in nucleons and nuclei are of great current interest. The modification of the parton distribution functions (PDFs) in the nuclear environment has attracted growing attention ever since the pioneering EMC experiment[1, 2]. At the Relativistic Heavy Ion Collider (RHIC), we are well-positioned to study the nuclear PDFs (nPDFs) in a center-of-mass energy and transverse-momentum domain where perturbative Quantum Chromodynamics (pQCD) is expected to work well. Thus, hadron production in nuclear collision experiments at RHIC should provide information on how such non-perturbative ingredients of pQCD as the parton distribution functions are modified by the presence of the nuclear medium.

However, the description of nuclear collisions based on pQCD is a complicated task. Much of the complication derives from the intrinsically complex nature of the nuclear environment in collisions of heavy nuclei. In addition to the initial-state modification of the PDFs, the cross section of high- $p_T$  hadron production is influenced by final-state effects (such as jet energy loss) and a complicated geometry. To better understand the physics of pQCD in the nuclear environment, it is highly desirable to disentangle the different nuclear phenomena affecting high- $p_T$  ( $p_T \gtrsim 2$  GeV/c) hadron production. These phenomena (not present in proton-proton collisions) manifest themselves in e.g. the measured nuclear modification factors.

Deuteron-gold (d+Au) collisions provide a good compromise and testing ground for these purposes. The deuteron, being the simplest “real” nucleus, affords a complexity higher than a proton, but much less than that of a typical heavy nucleus like gold. Thus, a good understanding of d+Au collisions is invaluable in elucidating the added complexity associated with collisions of more complex heavy nuclei. Accordingly, d+Au collisions have been extensively studied at RHIC (see e.g. [3, 4, 5, 6]). A new feature, offered by nonidentical colliding beams like d+Au, is the pseudorapidity asymmetry, examined

in some detail recently by the STAR collaboration[7].

Any pQCD calculation involves, in addition to partonic differential cross sections, parton distribution functions (PDFs) and fragmentation functions (FFs) to connect to the observable level. The latter ingredients are non-perturbative, but universal in the absence of the nuclear environment. Typical pQCD-based calculations of nucleus-nucleus collisions use modified (nuclear) PDFs and deal with issues like jet energy loss (jet quenching) and collision geometry. In this work, we focus on the PDFs (and of course can not avoid treating the geometry of the collision). Even in the proton (nucleon), our knowledge of the PDFs is naturally limited; the nPDFs are much less well known in the wide range of momentum fraction  $x$  needed for reliable calculations. The nuclear gluon distribution, in particular, is poorly constrained. The uncertainties in the nPDFs directly affect the accuracy of pQCD calculations. It is therefore important not to rely on a single nPDF parametrization. Calculations utilizing different parameterizations offer a useful check on the performances of the different nPDFs in describing relevant observables.

In the present work we compute nuclear modifications expressed in terms of the ratios  $R_{dAu}$  (nuclear modification factor, see eq. (8)) and  $R_{CP}$  (central-to-peripheral ratio, see eq. (11)). We also calculate the pseudorapidity asymmetry  $Y_{Asym}$  (see eq. (12)) in certain pseudorapidity intervals. We focus attention on the phenomenon of nuclear shadowing, the difference between PDFs and nPDFs, leaving aside possible additional effects like jet quenching or intrinsic parton transverse momentum and its broadening in nuclear collisions. In this way we establish a minimalist base line for experimental comparisons.

An earlier study along these lines [8] used the Eskola-Kolhinen-Salgado (EKS)[9] and Frankfurt-Guзей-Strikman (FGS)[10] parameterizations of nuclear shadowing. In Refs. [9, 10] the basic object is the shadowing function, which encodes the relevant nuclear information. The nPDFs are then a product of the shadowing function and nucleon PDFs. In our present study we are particularly interested in the Hirai-Kumano-Nagai (HKN) parameterization [11], which also gives the parton distribution functions for the deuteron, unlike other

parameterizations in which the deuteron is not shadowed. (Deuteron shadowing is of course a small effect compared to shadowing in heavy nuclei.) A short review of the available nuclear parton distribution functions and their differences can be found in Ref. [12]. Another point of departure in the present study from Ref. [8] is the use here of the Albino-Kramer-Kniehl (AKK) fragmentation functions [13]. These updated fragmentation functions are only available in next-to-leading order (NLO) and incorporate new experimental information from the OPAL Collaboration, including light quark tagging probabilities[14]. Thus AKK is expected to offer a better description of the fragmentation process. For calculations involving the EKS and FGS shadowing functions we need the nucleon parton distributions. We use the MRST2001 leading order (LO) PDFs[15] for consistency with HKN, where the underlying nucleon PDFs are the MRST2001 LO PDFs.

The paper is organized as follows: in Sec. II we review the basic formalism of LO pQCD as applied to d+Au collisions. This Section also includes the definitions of the nuclear modification factor, the central-to-peripheral ratio, and the pseudorapidity asymmetry, and a brief review of the available experimental data. We present the results of our calculation in Sec. III, and conclude in Sec. IV.

## II. BASIC FORMALISM

The invariant cross section for the d+Au  $\rightarrow$  h+X reaction, with respect to pseudorapidity  $\eta$  and transverse momentum  $p_T$  can be written as

$$\frac{d\sigma_{dAu}^h}{d\eta d^2p_T} = \sum_{abcd} \int d^2b d^2s dx_a dx_b dz_c t_d(\vec{s}) t_{Au}(|\vec{b} - \vec{s}|) F_{a/d}(x_a, Q^2, \vec{s}, z) F_{b/Au}(x_b, Q^2, |\vec{b} - \vec{s}|, z') \frac{d\sigma(ab \rightarrow cd)}{d\hat{t}} \frac{D_{h/c}(z_c, Q_f^2)}{\pi z_c^2} \hat{s} \delta(\hat{s} + \hat{t} + \hat{u}), \quad (1)$$

where  $x_a$  and  $x_b$  are parton momentum fractions in deuteron and gold, respectively, and  $z_c$  is the fraction of the parton momentum carried by the final-state hadron  $h$ . The factorization and fragmentation scales are  $Q$  and  $Q_f$ , respectively. Here,

$$t_A(\vec{s}) = \int dz \rho_A(\vec{s}, z) \quad (2)$$

is the Glauber thickness function of nucleus  $A$ , with the nuclear density distribution,  $\rho_A(\vec{s}, z)$  subject to the normalization condition

$$\int d^2s dz \rho_A(\vec{s}, z) = A. \quad (3)$$

The quantity  $d\sigma(ab \rightarrow cd)/d\hat{t}$  in eq. (1) represents the perturbatively calculable partonic cross section, and

$D_{h/c}(z_c, Q_f^2)$  stands for the fragmentation function of parton  $c$  to produce hadron  $h$ , evaluated at momentum fraction  $z_c$  and fragmentation scale  $Q_f$ . Using the  $\delta$ -function in eq. (1), the integration over  $z_c$  can be carried out explicitly. Integration limits over  $x_a$  and  $x_b$  are then  $(x_{amin}, 1)$  and  $(x_{bmin}(x_a), 1)$  respectively. Note that  $x_{bmin}$  is a function of  $x_a$ . In addition,  $z_c$  is also a function of both  $x_a$  and  $x_b$ .

In the present study, we are primarily concerned with  $F_{a/A}(x, Q^2, \vec{s}, z)$ , the nuclear parton distribution function (nPDF) for nucleus  $A$ . In light of the nuclear modifications discussed in Sec. I, it is natural to assume that the nPDF depends on the location of the parton in the nucleus,  $(\vec{s}, z)$  (or at least on its position relative to the beam axis  $\vec{s}$ ). To connect this ‘‘inhomogeneous’’ nPDF to the geometry-independent (homogeneous) nPDF  $\mathcal{F}_{a/A}(x, Q^2)$ , the normalization condition

$$\int d^2s dz \rho_A(\vec{s}, z) F_{a/A}(x, Q^2, \vec{s}, z) = \mathcal{F}_{a/A}(x, Q^2) \quad (4)$$

should be satisfied.

In the EKS[9], FGS[10], and HIJING[16] parameterizations the (homogeneous) shadowing function  $\mathcal{S}(x, Q^2)$  is introduced, and the nPDF is written as

$$\mathcal{F}_{a/A}(x, Q^2) = \mathcal{S}(x, Q^2) f_{a/N}(x, Q^2), \quad (5)$$

where  $f_{a/N}(x, Q^2)$  is the PDF of the nucleon, which can be expressed as

$$f_{a/N}(x, Q^2) = \frac{Z}{A} f_{a/p}(x, Q^2) + (1 - \frac{Z}{A}) f_{a/n}(x, Q^2), \quad (6)$$

with  $f_{a/p}(x, Q^2)$  [ $f_{a/n}(x, Q^2)$ ] being the proton [neutron] parton distribution function as a function of Bjorken  $x$  and factorization scale  $Q$ . The HKN parameterization is already given in terms of nPDFs.

Especially at small values of  $x$ , where coherence effects are important, scaling with the thickness function appears to be more physical than with the local density. Therefore, in this work we assume that shadowing is proportional to the thickness function (2) (i.e. we adopt the second option discussed in Ref. [8]).

The connection between the inhomogeneous and homogeneous shadowing functions,  $S_A(x, Q^2, \vec{s}, z)$  and  $\mathcal{S}(x, Q^2)$ , respectively, can be written as

$$S_A(x, Q^2, \vec{s}, z) = 1 + N[\mathcal{S}(x, Q^2) - 1] \frac{\int dz \rho_A(\vec{s}, z)}{\int dz \rho_A(0, z)}, \quad (7)$$

with  $N$  a normalization constant. In other words, the deviation of the inhomogeneous shadowing function from unity is proportional to the deviation from unity of the homogeneous shadowing function and proportional to the thickness function. While inhomogeneous FGS nPDFs are available, for consistency and ease of comparison with EKS and HKN, we apply the homogeneous FGS nPDFs.

We obtain the density distribution of the deuteron from the Hulthen wave function[17] (as in Ref. [18]),

while a Woods-Saxon density distribution is used for gold with parameters from Ref. [19]. Since the Nijmegen deuteron wave function[20], which we also applied, gives similar results to the Hulthen wave function, we report only the calculations using the Hulthen wave function here.

We fix the scales as  $Q = Q_f = p_T$ , where  $p_T$  is the final hadronic transverse momentum. We also carried out calculations with the scales  $Q = p_T/z_c$ ,  $Q_f = p_T$ . Results with the latter choice do not differ significantly from those obtained by having both scales fixed at  $p_T$ . The partonic differential cross sections,  $d\sigma(ab \rightarrow cd)/d\hat{t}$  were evaluated at leading order (LO). We note that, if a  $K$  factor was used to approximate the effects of higher orders, these effects would cancel in the ratios calculated in the present study. For the fragmentation functions we use the AKK set[13] throughout.

### A. Nuclear Modification Factors

The d+Au nuclear modification factor,  $R_{dAu}$  is defined as

$$R_{dAu}(p_T) = \frac{1}{\langle N_{bin} \rangle} \frac{d\sigma_{dAu}^h}{d\eta d^2p_T} \bigg/ \frac{d\sigma_{pp}^h}{d\eta d^2p_T} , \quad (8)$$

where the average number of binary collisions,  $\langle N_{bin} \rangle$  in the various impact-parameter bins is given by

$$\langle N_{bin} \rangle = \langle \sigma_{NN}^{in} T_{dAu}(b) \rangle . \quad (9)$$

Here  $\sigma_{NN}^{in}$  is the inelastic nucleon-nucleon cross section, and

$$T_{dAu}(b) = \int d^2s t_d(\vec{s}) t_{Au}(|\vec{b} - \vec{s}|) \quad (10)$$

represents the deuteron-gold nuclear overlap function. The nuclear modification factor  $R_{dAu}$  is thus just the ratio of the d+Au and proton-proton (pp) cross sections, normalized by the average number of binary collisions,  $\langle N_{bin} \rangle$ .

### B. Central-to-Peripheral Ratios

A related ratio, which dispenses with the need for a reference pp cross section and uses information from the same experiment in numerator and denominator, thus canceling most systematic errors, is the central to peripheral ratio defined as

$$R_{CP}(p_T) = \frac{1}{\langle N_{bin} \rangle_C} \frac{d\sigma_{dAu}^{hC}}{d\eta d^2p_T} \bigg/ \frac{1}{\langle N_{bin} \rangle_P} \frac{d\sigma_{dAu}^{hP}}{d\eta d^2p_T} , \quad (11)$$

where  $\langle N_{bin} \rangle$  is as defined above. The label  $C$  stands for the central event class, while  $P$  denotes the peripheral class. The centrality classes are chosen according to centrality cuts on the experimental data.

The nuclear modification factors  $R_{dAu}$  have been measured at several pseudorapidities by the BRAHMS Collaboration, and are presented at  $|\eta| \leq 0.2$  ( $\eta = 0$ ),  $0.8 \leq \eta \leq 1.2$  ( $\eta = 1$ ),  $1.9 \leq \eta \leq 2.35$  ( $\eta = 2.2$ ), and  $2.9 \leq \eta \leq 3.5$  ( $\eta = 3.2$ )[5]. At small rapidities ( $\eta = 0, 1$ ), the data are given for the sum of charged hadrons, while at forward rapidities negatively charged hadron data are available. The AKK fragmentation functions are for average charged hadrons. It should be remembered that the calculated results for all rapidities are therefore for the average of charged hadrons. Furthermore, the BRAHMS data are given in three centrality classes: central (0-20)%, semicentral (30-50)%, and peripheral (60-80)% (as a percentile of the geometric cross section). With a Woods-Saxon density for gold and the Hulthen wave function for the deuteron, a Glauber calculation of  $T_{dAu}$  relates these classes to impact parameter intervals as[8]  $0 \leq b \leq 3.81$  fm for central,  $4.66 \leq b \leq 6.01$  fm for semicentral, and  $6.59 \leq b \leq 7.74$  fm for peripheral. We will use the notation  $R_{CP}$  to refer to the central-to-peripheral ratio, while  $R_{SP}$  will be used to denote the semicentral-to-peripheral ratio in the following.

### C. Pseudorapidity Asymmetry

As the mechanisms for hadron production in d+Au collisions may be different at forward rapidities (deuteron side) and backward rapidities (gold side), it is of interest to study ratios of particle yields between a given rapidity value and its negative in these collisions. The STAR Collaboration has recently measured pseudorapidity asymmetries[7], defined as

$$Y_{Asym} = \frac{d\sigma_{dAu}^h}{d\eta d^2p_T}(\text{Au-side}) \bigg/ \frac{d\sigma_{dAu}^h}{d\eta d^2p_T}(\text{d-side}) , \quad (12)$$

in d+Au collisions for several identified hadron species and total charged hadrons in the pseudorapidity intervals  $|\eta| \leq 0.5$  and  $0.5 \leq |\eta| \leq 1.0$ . Rapidity asymmetries with the backward/forward ratio above unity for transverse momenta up to  $\approx 5$  GeV/c are observed for charged pion, proton+anti-proton, and total charged hadron production in both rapidity regions. We want to see if different nPDFs give significantly different rapidity asymmetries for the various hadron species.

## III. RESULTS

Before presenting the results from the three different nPDFs, we note that while EKS and HKN are similar in the sense that they are global fits to experimental data, FGS is relying on Gribov theory for diffractive deep inelastic scattering to derive nPDFs. Gluon shadowing is much stronger in FGS than in EKS and HKN. Because nuclear gluon distributions are poorly constrained experimentally, there are significant differences between the

EKS and HKN gluon shadowing. On the other hand, since the Gribov formalism is not capable to predict valence quark shadowing, FGS uses EKS shadowing for valence quarks, and all three parameterizations are in agreement for valence quark shadowing. For sea quarks, EKS and HKN are in good agreement at  $0.01 \lesssim x \lesssim 0.1$ . At  $x \gtrsim 0.2$  and in the small- $x$  region  $x \lesssim 0.01$  there are substantial deviations. The FGS predicts more nuclear shadowing for sea quarks than EKS and HKN. Due to the  $x$ -integration, different nuclear effects [shadowing ( $x \lesssim 0.1$ , depletion), antishadowing ( $0.1 \lesssim x \lesssim 0.3$ , enhancement), EMC effect ( $0.3 \lesssim x \lesssim 0.7$ , depletion), etc] are superimposed, thus it is difficult to isolate these effects.

Since pQCD calculations are generally not reliable at low  $p_T$ , we do not wish to push our calculations below  $p_T = 1.5$  GeV/c. With our scale choice, this corresponds to a minimum  $Q^2$  ( $Q_f^2$ ) of  $2.25$  GeV<sup>2</sup>, while EKS, FGS, and HKN give  $2.25, 4.0$ , and  $1.0$  GeV<sup>2</sup> for minimum  $Q^2$ , respectively. The minimum  $Q_f^2$  for the AKK fragmentation functions is given as  $2.0$  GeV<sup>2</sup>.

### A. Nuclear Modification Factors

We have calculated the minimum bias  $R_{dAu}$  for total charged hadron production at the BRAHMS pseudorapidities with the three nuclear parton distribution functions considered in this study. In the case of the FGS nPDFs we use the strong gluon shadowing for the gold nucleus. We have only calculated the  $p_T$  distributions for final-state total charged hadrons in the present study, since we are mainly interested in the performance of the different nPDFs. More detail for different hadron species and fractional contributions from quarks, antiquarks, and gluons for EKS and FGS nPDFs can be found in [8]. Here we limit our discussion of nuclear modification factors to the effect of the different nPDFs. We make two general observations:

- i) At midrapidity (small  $\eta$ ), processes initiated by both gluons and quarks are important. At forward rapidities (large  $\eta$ ),  $x_b$ , the parton momentum fraction in gold becomes small and gluon-initiated processes become dominant.
- ii) In both, the data and the calculations,  $R_{dAu}$  decreases systematically with increasing  $\eta$ . This reflects the increasing role of shadowing since smaller values of  $x_b$  are probed at forward rapidities.

The results of our calculations are displayed in Fig. 1, together with the experimental data. At  $\eta = 0$  and  $p_T = 1.5$  GeV/c, typical  $x_{min}$  values are significantly below  $0.1$ . Thus there is substantial contribution from the shadowing region, and all three nPDFs predict  $R_{dAu} < 1$ , with the HKN being the lowest. Due to their steeper rise of  $R_{dAu}$  with  $p_T$ , the EKS and FGS nPDFs appear to describe the data better at around  $p_T = 3$  GeV/c than the

HKN nPDFs. At  $p_T = 4$  GeV/c,  $x_{bmin}$  is above  $0.5$  for some values of  $x_a$ . There is thus more contribution from the antishadowing region, and consequently  $R_{dAu} > 1$ , with the HKN still being the lowest. At  $p_T = 8$  GeV/c, we have major contributions from both antishadowing and the EMC effect. Thus, while  $R_{dAu}$  is still  $> 1$ , the trend is towards  $1$  for both EKS and FGS. The HKN parameterization predicts a higher value at around  $1.1$ .

The behavior is similar at  $\eta = 1$ . At  $p_T = 1.5$  GeV/c both  $x_{min}$  values are small, and thus  $R_{dAu} < 1$ . Around this  $p_T$  the HKN is identical with the FGS. At  $p_T = 4$  GeV/c,  $x_{bmin}$  ranges higher, with  $R_{dAu} > 1$ . The HKN is slightly below both EKS and FGS in this region. At  $p_T = 8$  GeV/c,  $R_{dAu} > 1$  with substantial contributions from both antishadowing and the EMC effect. The HKN is practically the same as EKS and slightly higher than FGS. All three are in good agreement with data except at low  $p_T$ , where the data are more suppressed than the calculated results.

The effect of increasing  $\eta$  is already apparent at  $\eta = 2.2$ , where both FGS and HKN are below unity for all  $p_T$  considered. The EKS is practically  $1$  at mid- $p_T$  and falls below  $1$  at high  $p_T$ . The major contribution is from shadowing with the resultant  $R_{dAu} < 1$ . Note that at low  $p_T$  the HKN is similar to the EKS, while at higher  $p_T$  it is lower than both EKS and FGS. The agreement with data is reasonable.

At  $\eta = 3.2$  the dominant contribution is again from shadowing with  $R_{dAu} < 1$  for all  $p_T$ . At low  $p_T$  the FGS describes the data best while at high  $p_T$  it is similar to the EKS. This may be due to the stronger gluon shadowing in the FGS. The HKN is less suppressed at low  $p_T$  than both EKS and FGS, while at higher  $p_T$  it is more suppressed than the others..

### B. Central-to-Peripheral Ratios

The results of our central-to-peripheral ratio ( $R_{CP}$ ) calculation are displayed in Fig. 2, together with the BRAHMS data. At  $\eta = 0$ , where the data indicate an  $R_{CP} > 1$  at  $2 \lesssim p_T \lesssim 4$  GeV/c, the calculated results are below the data, while at both  $\eta = 2.2$  and  $\eta = 3.2$  the data show significant suppression, with the calculations giving  $R_{CP}$  close to unity. At  $\eta = 1$  the calculation can be said to be in reasonable agreement with the data. Although the calculation exhibits the trend toward increasing suppression in the data as  $\eta$  increases, the calculated variation with  $\eta$  is much smaller than the one shown by the data. This shortcoming becomes increasingly evident at forward rapidities. Fig. 3 shows the calculated semicentral-to-peripheral ratio,  $R_{SP}$ , using the three nPDFs, together with the BRAHMS data. The situation here mirrors that of the central-to-peripheral ratios. The results underpredict the data at  $\eta = 0$ , but overpredict at forward rapidities. The degree of suppression at forward rapidities is not as severe as in the central-to-peripheral ratios. In fact, due to the large error bars,

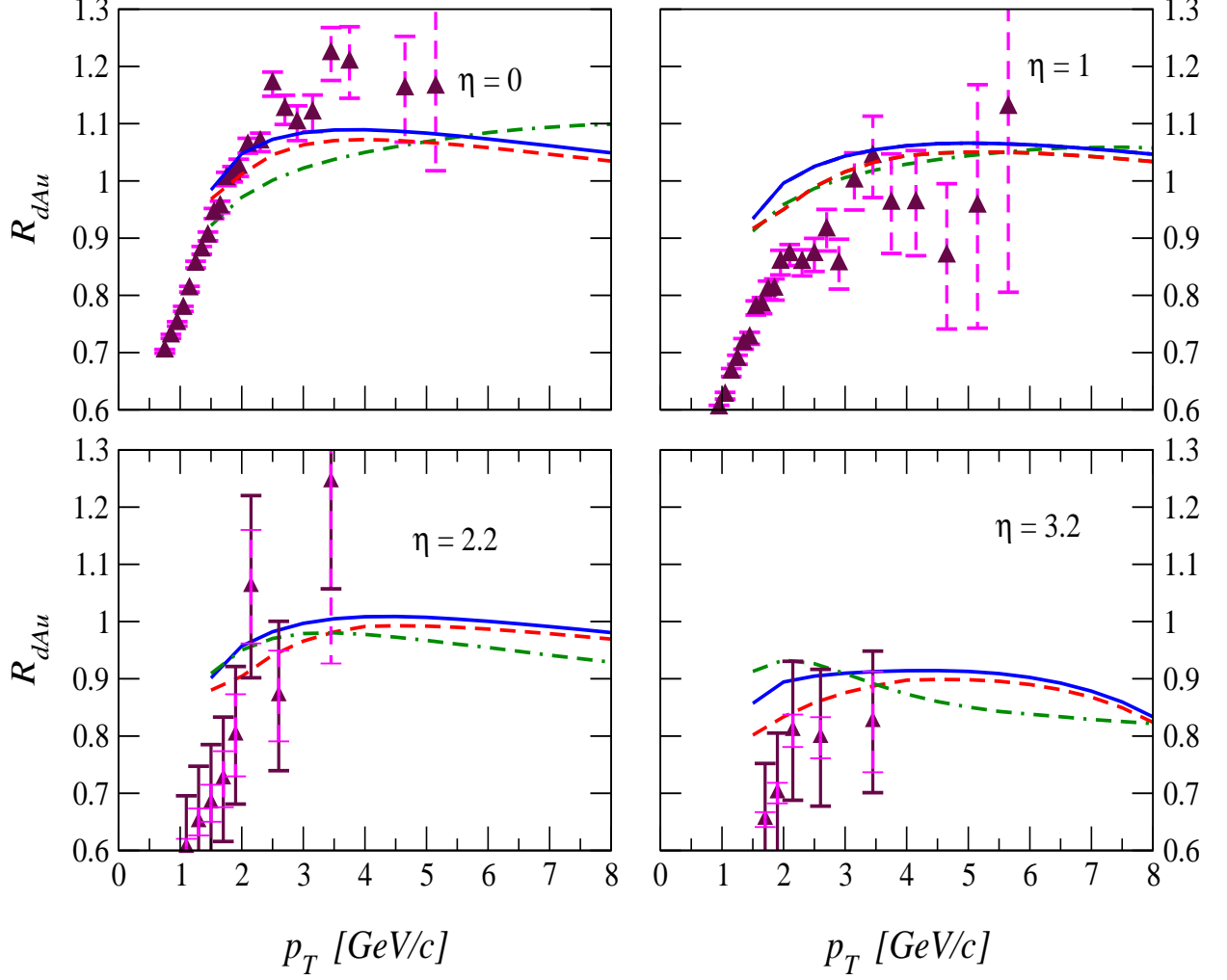


FIG. 1: (Color Online) Minimum bias nuclear modification factor  $R_{dAu}$  for total charged hadron production at different pseudorapidities, using EKS (solid), FGS (dashed), and HKN (dot-dashed) nPDFs. Solid triangles denote BRAHMS data. In the top panels the data are for average charged hadrons, while for the bottom panels only negative hadrons are measured. The solid error bars are systematic errors, while dashed error bars represent statistical errors. For clarity, only statistical errors are displayed in the two upper panels, where the systematic errors are rather large.

there is reasonable agreement with data at  $p_T$  around 4 GeV/c.

Both  $R_{CP}$  and  $R_{SP}$  are geometry-dependent, thus the assumed spatial dependence of shadowing is important. We have checked that shadowing proportional to the local density gives worse agreement with data than shadowing proportional to the thickness function. A variation of the thickness function dependence where we used

higher powers gives better agreement at  $\eta = 0$  but still overpredicts significantly at other rapidities. With these shadowing parameterizations, a more radical spatial dependence is needed to describe the data for both ratios. Another factor that may be responsible is a too-weak  $x$ -dependence of the available shadowing parameterizations.

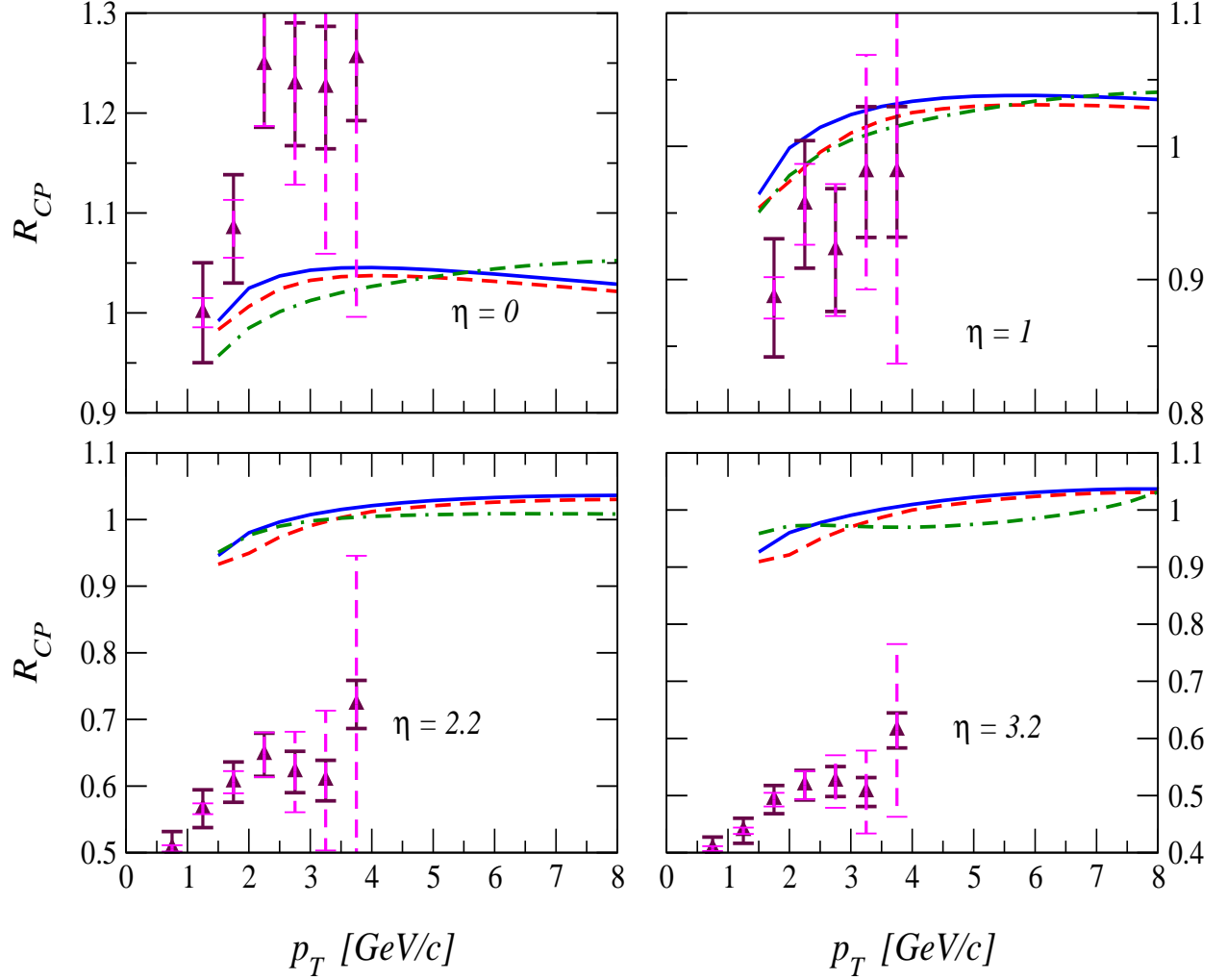


FIG. 2: (Color Online) Central-to-peripheral ratio  $R_{CP}$  for total charged hadron production at different pseudorapidities using EKS (solid), FGS (dashed), and HKN (dot-dashed) nPDFs. Solid triangles denote BRAHMS data. The solid error bars are systematic errors, while dashed error bars represent statistical errors.

### C. Pseudorapidity Asymmetry

In d+Au collisions at small rapidities, particle production may include contributions from gold-side partons that may have been modified by nuclear effects and from deuteron-side partons that have experienced multiple scatterings while traversing the gold nucleus [7]. It should be kept in mind that the latter effect is not included in the present calculations.

We have calculated  $Y_{asym}$  for charged pions ( $\pi^+ + \pi^-$ ),

charged kaons, protons+antiprotons ( $p + \bar{p}$ ), and total charged hadrons ( $h^+ + h^-$ ). Below 2 GeV/c, data are available for total charged hadrons only. Above 2 GeV/c, separated data exist for  $\pi^+ + \pi^-$  and for  $p + \bar{p}$ . A benefit of using a ratio is that the systematic errors largely cancel and are  $\lesssim 5\%$  for both pions and protons,  $< 3\%$  for charged hadrons [7]. For  $p_T \lesssim 4.2$  GeV/c the errors are dominantly systematic and thus the statistical errors are not displayed. At higher  $p_T$  statistical errors tend to become dominant. Since the asymmetry is a ratio of

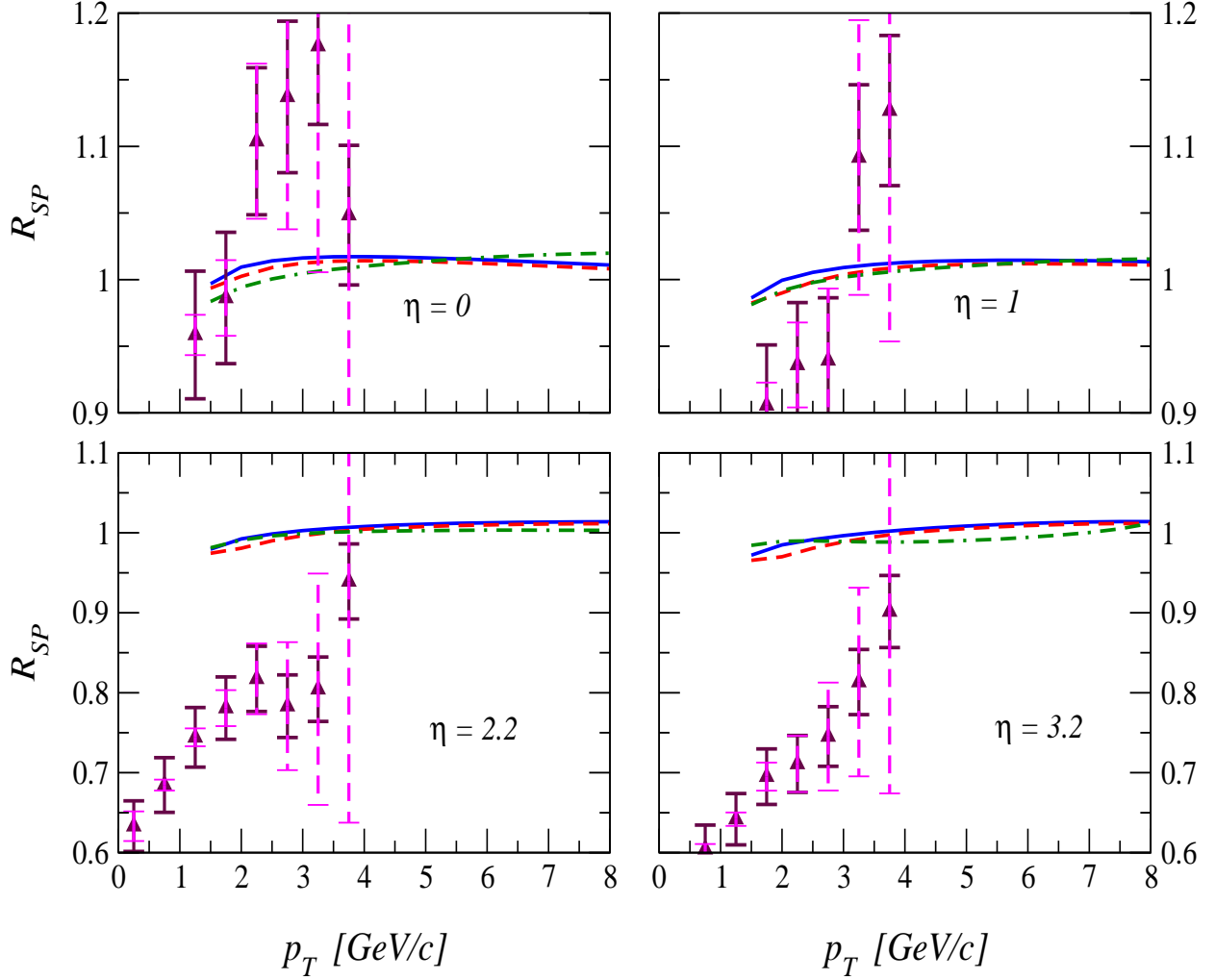


FIG. 3: (Color Online) Semicentral-to-peripheral ratio  $R_{SP}$  for total charged hadron production at different pseudorapidities using EKS (solid), FGS (dashed), and HKN (dot-dashed) nPDFs. Solid triangles denote BRAHMS data. The solid error bars are systematic errors, while dashed error bars represent statistical errors.

the yields in two different rapidity intervals, the respective  $x_b$ -distributions are mostly responsible for the global trends observed in the calculations.

Fig. 4 shows the result of our pseudorapidity asymmetry ratio calculations for the interval  $|\eta| \leq 0.5$ , together with the STAR data[7]. We plot the calculated results with the EKS (solid line), FGS (dashed), and HKN (dot-dashed) nuclear parton distributions. Around  $\eta = 0$  one expects the degree of asymmetry to be small. This is borne out by both data and calculation. At very low

$p_T$ , there is more contribution from the shadowing region for the positive rapidity (deuteron-side) than the negative rapidity (gold-side). Thus the ratio is expected to be above unity. For  $p_T > 3$  GeV/c, the  $x_b$  distributions are similar, with less contribution from the shadowing region as  $p_T$  increases. Thus the asymmetry is not far from unity. The EKS and FGS nPDFs give similar results for all hadronic species. The HKN nPDFs yield a different curvature and pseudorapidity asymmetries that remain above unity for a wider range of transverse momenta.

For the total charged hadrons ratio, the calculation is below the data for  $p_T \lesssim 5$  GeV/c. At the present level of combined experimental and theoretical uncertainties, we can claim that  $Y_{asym}$  is reasonably reproduced for  $\pi^+ + \pi^-$  and  $p + \bar{p}$ , in particular at large transverse momenta. The EKS and FGS predictions for charged kaons have a small maximum at  $p_T \approx 2.2$  GeV/c.

Figure 5 shows the result of our pseudorapidity asymmetry ratio calculations for the interval  $0.5 \leq |\eta| \leq 1.0$ . At low  $p_T$ , the situation is similar to  $|\eta| \leq 0.5$ . Thus the asymmetry is above unity. However, at  $p_T > 3$  GeV/c, the  $x_b$  distributions start to become significantly different. While there are still some contributions from the shadowing region for the positive rapidity even up to the highest  $p_T$ , the negative rapidity yield has no shadowing contribution for  $p_T \gtrsim 8$  GeV/c. Thus one expects the asymmetry to be more substantial than for  $|\eta| \leq 0.5$ . This is borne out by the calculations. As in  $|\eta| \leq 0.5$ , EKS and FGS give very similar results. The HKN nPDFs also behave similarly to what was seen at  $|\eta| \leq 0.5$ , the difference between EKS and FGS on the one side, and HKN on the other, becoming more pronounced. All calculations underpredict the data for  $h^+ + h^-$ . For  $\pi^+ + \pi^-$  and  $p + \bar{p}$ , the calculation agrees with the data within error for large transverse momenta. It will be interesting to see the data for charged kaons, when they become available[21].

#### IV. CONCLUSION

We have calculated nuclear modification factors  $R_{dAu}$  in deuteron-gold collisions at  $\sqrt{s} = 200$  GeV using three nuclear shadowing parameterizations: the EKS, FGS, and HKN nuclear parton distribution functions. We have also calculated a related modification factor, the central-

to-peripheral ratio,  $R_{CP}$ , using the impact parameter representation of the BRAHMS centrality classes. We have used the AKK fragmentation functions throughout in our calculations.

All three nPDFs give similar results for the minimum bias  $R_{dAu}$  at forward rapidities. For not too large rapidities and relatively low  $p_T$ , the HKN values are smaller than those of the EKS and FGS. The calculated results for all three nPDFs approximately agree with the data.

The  $R_{CP}$  results do not describe the data well overall. At  $|\eta| \leq 0.2$  the calculated results underestimate the data, while at the most forward rapidities the data are much below the calculated results. Only at  $\eta = 1$  can we claim approximate agreement with data, but this appears to be coincidental, judging from the  $\eta$ -dependence of the data and the calculated results. This situation may be due to poor knowledge of the spatial dependence of nuclear shadowing. It may also signify a rapidity dependence of shadowing.

For all hadronic species the calculated pseudorapidity asymmetry underestimates the data for  $p_T \lesssim 5$  GeV/c. At higher  $p_T$ , EKS and FGS results tend to fall lower than unity, while HKN yields values above one. Present uncertainties in the experimental data do not allow a distinction between these scenarios. We expect further data up to higher transverse momenta and with smaller uncertainties in the near future for all the observables discussed here.

#### V. ACKNOWLEDGMENTS

This work was partly supported by the U.S. Department of Energy under grant U.S. DE-FG02-86ER40251. We thank V. Guzey for stimulating discussions and B. Mohanty for information on experimental errors.

- 
- [1] J. J. Aubert *et al.* [European Muon Collaboration], Phys. Lett. B **123**, 275 (1983).
  - [2] D. F. Geesaman, K. Saito and A. W. Thomas, Ann. Rev. Nucl. Part. Sci. **45**, 337 (1995).
  - [3] S.S. Adler *et al.* [PHENIX Collaboration], Phys. Rev. Lett. **91**, 072303 (2003); Phys. Rev. **C74**, 024904 (2006).
  - [4] J. Adams *et al.* [STAR Collaboration], Phys. Rev. Lett. **91**, 072304 (2003); Phys. Rev. **C70**, 064907 (2004).
  - [5] I. Arsene *et al.* [BRAHMS Collaboration], Phys. Rev. Lett. **93**, 242303 (2004).
  - [6] H. Yang, [BRAHMS Collaboration], arXiv:nucl-ex/0702004.
  - [7] B. I. Abelev *et al.* [STAR Collaboration], arXiv:nucl-ex/0609021. J. Adams *et al.* [STAR Collaboration], Phys. Rev. C **70**, 064907 (2004).
  - [8] R. Vogt, Phys. Rev. C **70**, 064902 (2004).
  - [9] K. J. Eskola, V. J. Kolhinen and C. A. Salgado, Eur. Phys. J. C **9**, 61 (1999).
  - [10] L. Frankfurt, V. Guzey and M. Strikman, Phys. Rev. D **71**, 054001 (2005).
  - [11] M. Hirai, S. Kumano, and T.-H. Nagai, Phys. Rev. **C70**, 044905 (2004); Nucl. Phys. B Proc. Suppl. **139**, 21 (2005).
  - [12] V. J. Kolhinen, Phys. Rev. D **66**, 010001 (2002).
  - [13] S. Albino, B. A. Kniehl and G. Kramer, Nucl. Phys. B **725**, 181 (2005).
  - [14] G. Abbiendi *et al.* [OPAL Collaboration], Eur. Phys. J. C **16**, 407 (2000).
  - [15] A. D. Martin, R. G. Roberts, W. J. Stirling and R. S. Thorne, Eur. Phys. J. C **23**, 73 (2002).
  - [16] S. y. Li and X. N. Wang, Phys. Lett. B **527**, 85 (2002).
  - [17] L. Hulthen and M. Sugawara, "Handbuch der Physik", vol. 39 (1957).
  - [18] D. Kharzeev, E. Levin and M. Nardi, Nucl. Phys. A **730**, 448 (2004) [Erratum-ibid. A **743**, 329 (2004)].
  - [19] C. W. De Jager, H. De Vries and C. De Vries, Atom. Data Nucl. Data Tabl. **14**, 479 (1974).
  - [20] <http://nn-online.org>
  - [21] N. Xu, private communication (2007).



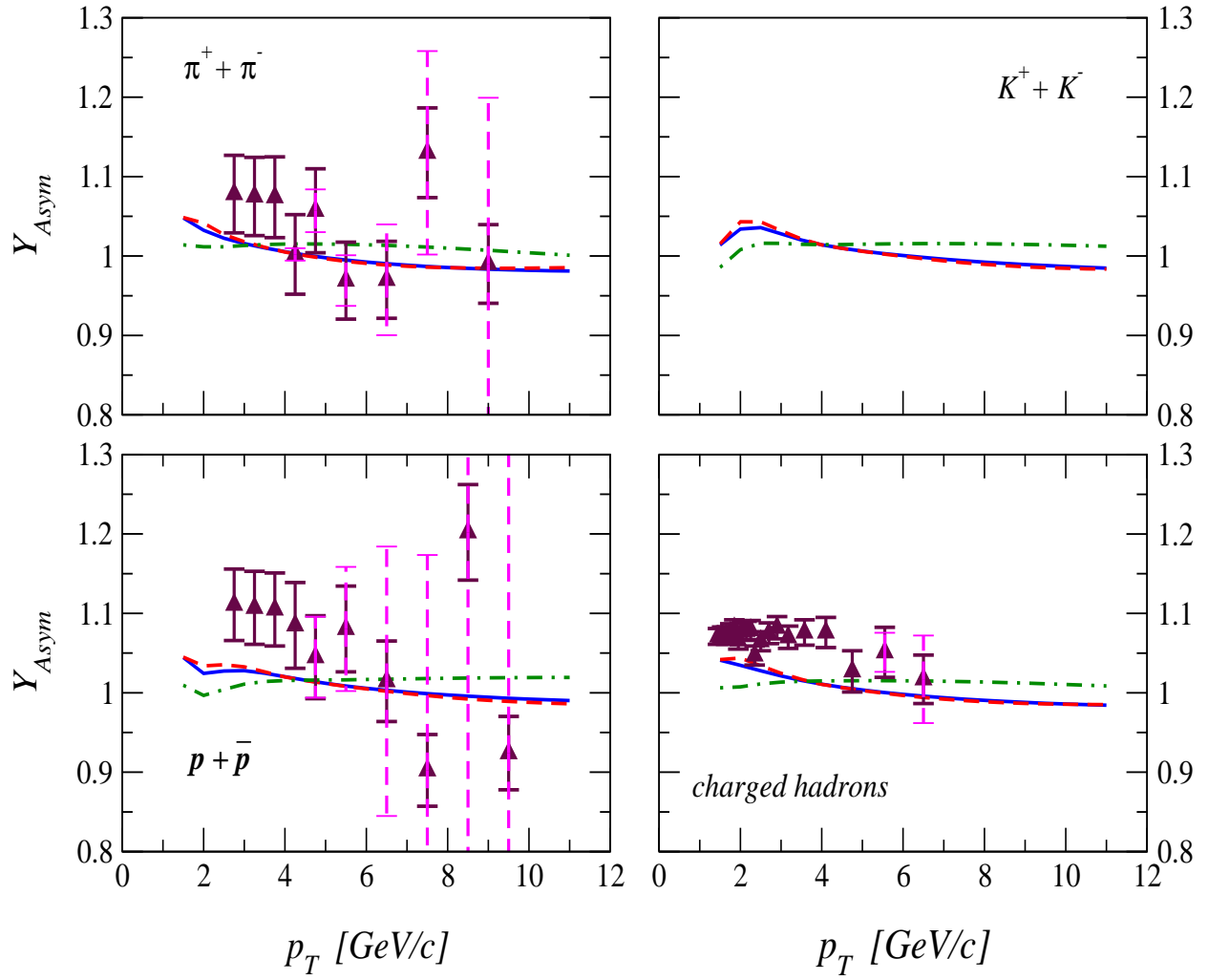


FIG. 4: (Color Online) Pseudorapidity asymmetry,  $Y_{asym}$  for different hadrons at  $|\eta| \leq 0.5$ . The solid line represents the EKS nPDFs while the dashed line is obtained with the FGS nPDFs. The dot-dashed line corresponds to the HKM nPDFs, and filled triangles denote the STAR data. The solid error bars are systematic errors, while dashed error bars represent statistical errors.

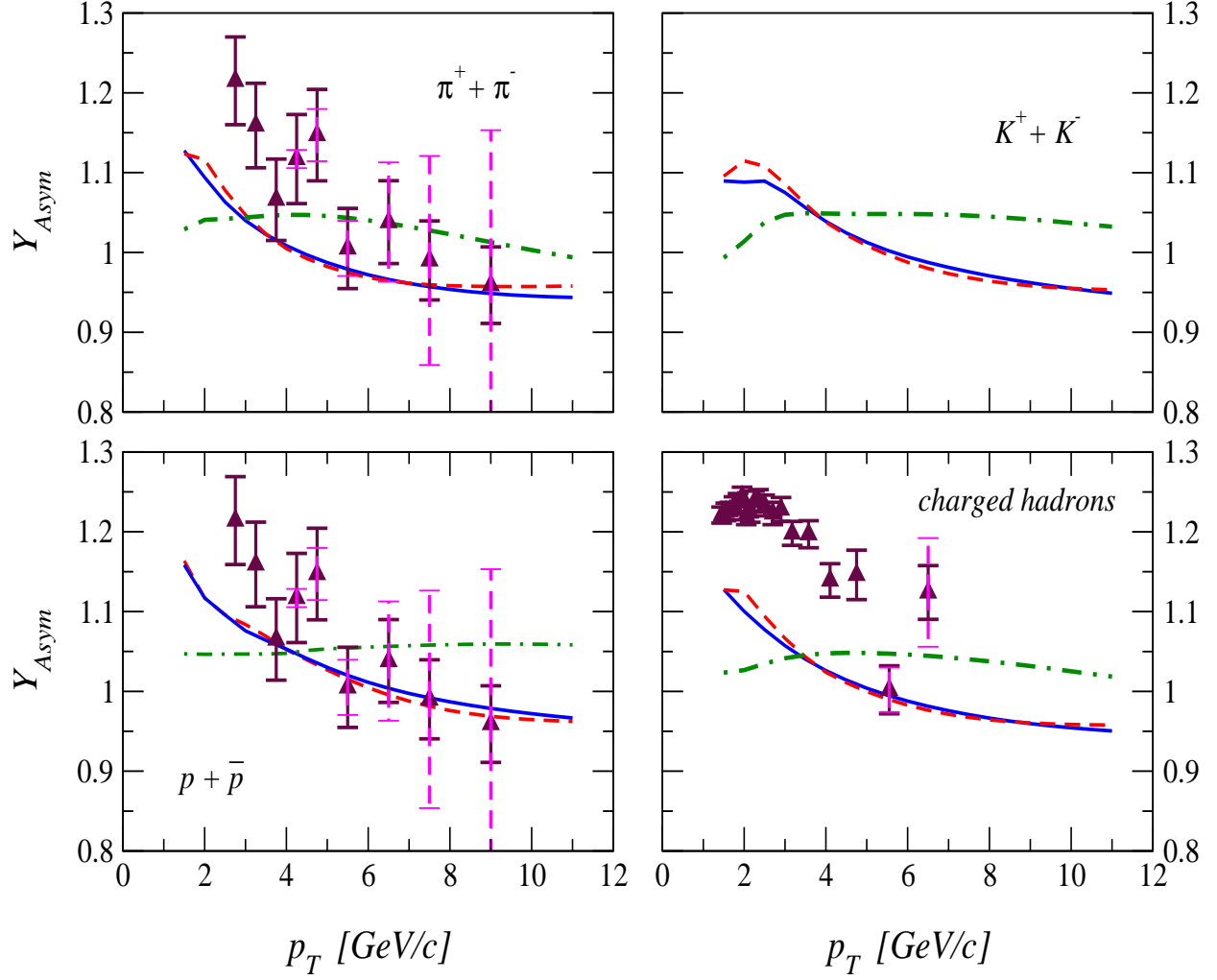


FIG. 5: (Color Online) Pseudorapidity asymmetry,  $Y_{asym}$  for different hadrons at  $0.5 \leq |\eta| \leq 1.0$ . The solid line uses EKS nPDFs, while the dashed line is obtained with the FGS nPDFs. The dot-dashed line corresponds to the HKN nPDFs, and filled triangles denote the STAR data. The solid error bars are systematic errors, while dashed error bars represent statistical errors.